IBRO Reports 2 (2017) 14–23

Contents lists available at ScienceDirect

IBRO Reports

journal homepage: http://www.journals.elsevier.com/ibro-reports

TBI-induced nociceptive sensitization is regulated by histone acetylation

De-Yong Liang [a, b, *], Peyman Sahbaie [a, b], Yuan Sun [a, b], Karen-Amanda Irvine [a, b], Xiaoyou Shi [a, b], Anders Meidahl [b], Peng Liu [a], Tian-Zhi Guo [a], David C. Yeomans [b], J. David Clark [a, b, *]

[a] Department of Anesthesiology, Veterans Affairs Palo Alto Health Care System, Palo Alto, CA, 3801 Miranda Ave, 94304, USA
[b] Department of Anesthesiology, Pain and Perioperative Medicine, Stanford University School of Medicine, Stanford, CA, 94305, USA

ARTICLE INFO

Article history:
Received 22 November 2016
Accepted 21 December 2016

Keywords:
Traumatic brain injury
Epigenetic regulation
Biomarker
Curcumin
Histone acetyltransferase
Histone deacetylase

ABSTRACT

Chronic pain after traumatic brain injury (TBI) is very common, but the mechanisms linking TBI to pain and the pain-related interactions of TBI with peripheral injuries are poorly understood. In these studies we pursued the hypothesis that TBI pain sensitization is associated with histone acetylation in the rat lateral fluid percussion model. Some animals received hindpaw incisions in addition to TBI to mimic polytrauma. Neuropathological analysis of brain tissue from sham and TBI animals revealed evidence of bleeding, breakdown of the blood brain barrier, in the cortex, hippocampus, thalamus and other structures related to pain signal processing. Mechanical allodynia was measured in these animals for up to eight weeks post-injury. Inhibitors of histone acetyltransferase (HAT) and histone deacetylase (HDAC) were used to probe the role of histone acetylation in such pain processing. We followed serum markers including glial fibrillary acidic protein (GFAP), neuron-specific enolase 2 (NSE) myelin basic protein (MBP) and S100β to gauge TBI injury severity. Our results showed that TBI caused mechanical allodynia in the hindpaws of the rats lasting several weeks. Hindpaws contralateral to TBI showed more rapid and profound sensitization than ipsilateral hindpaws. The inhibition of HAT using curcumin 50 mg/kg s.c reduced mechanical sensitization while the HDAC inhibitor suberoylanilide hydroxamic acid 50 mg/kg i.p. prolonged sensitization in the TBI rats. Immunohistochemical analyses of spinal cord tissue localized changes in the level of acetylation of the H3K9 histone mark to dorsal horn neurons. Taken together, these findings demonstrate that TBI induces sustained nociceptive sensitization, and changes in spinal neuronal histone proteins may play an important role.

© 2017 The Authors. This is an open access article under the CC BY-NC-ND license (http://creativecommons.org/licenses/by-nc-nd/4.0/).

1. Introduction

Traumatic brain injury (TBI) is a leading cause of death and disability worldwide, affecting all ages and demographics (Hyder et al., 2007). In the United States alone, approximately 1.7 million new cases are reported annually (Coronado et al., 2011; Faul and Coronado, 2015). While the vast majority of these injuries are mild, even these have been associated with a number of adverse consequences. These include memory impairment, anxiety, depression and other changes with variable patterns of onset and persistence (Murphy and Carmine, 2012; Rao et al., 2015). One of the most common complaints of patients after TBI is, however, chronic pain; it has been estimated that more than 50% of TBI patients develop chronic pain at some point after their injuries (Nampiaparampil, 2008). TBI was observed to confer an odds ratio of 5.0 for chronic pain in a recently described military cohort (Higgins et al., 2014). Unlike some of the more severe motor and cognitive consequences, chronic pain after TBI appears to be at least as likely to be experienced by those with mild as opposed to severe injuries (Nampiaparampil, 2008).

While the overall prevalence of chronic pain after TBI is high, the anatomical distribution of those symptoms is very broad. The most

* Corresponding authors. Department of Anesthesiology, Pain and Perioperative Medicine, Stanford University School of Medicine, Stanford, CA, 94305, USA.
E-mail addresses: dyliang@stanford.edu (D.-Y. Liang), psahbaie@stanford.edu (P. Sahbaie), yuansun@gmail.com (Y. Sun), karen.amanda.irvine@gmail.com (K.-A. Irvine), xshi@stanford.edu (X. Shi), anders@meidahl.dk (A. Meidahl), tianmittmm66@163.com (P. Liu), wxtguo@yahoo.com (T.-Z. Guo), dcyeomans@stanford.edu (D.C. Yeomans), djclark@stanford.edu (J.D. Clark).

http://dx.doi.org/10.1016/j.ibror.2016.12.001
2451-8301/© 2017 The Authors. This is an open access article under the CC BY-NC-ND license (http://creativecommons.org/licenses/by-nc-nd/4.0/).

commonly reported painful areas include the head, spine, limbs, and chest; amongst those with pain, limb pain is experienced by more than one-third of TBI patients (Mittenberg et al., 1992; Lahz and Bryant, 1996). Moreover, greater than 80% of polytrauma patients suffering from both TBI and peripheral injury report ongoing pain (Sayer et al., 2009). Relatedly, TBI worsens the functional outcomes of injuries to the extremities (Andruszkow et al., 2013).

Although only limited experimentation has been conducted, we are beginning to define the interactions of TBI with pain signaling pathways using laboratory models. For example, reduced periorbital and forepaw mechanical nociceptive thresholds were observed in both rats and mice using the Controlled Cortical Impact (CCI) model of TBI (Macolino et al., 2014). Recently Mustafa et al. used a closed-head TBI model in rats to demonstrate that multiple centers in the trigeminal sensory system (TSS) showed changes in the expression of pain-related genes. Correlations between changes in NK1 receptor expression and 5-HT fiber density with facial nociceptive sensitization were noted (Mustafa et al., 2016). An additional report from our laboratory showed hindpaw sensitization in rats after TBI using the Lateral Fluid Percussion (LFP) model as well as changes in spinal levels of brain derived neurotrophic factor (BDNF), a pain signaling related neurotrophin (Feliciano et al., 2014). The involvement of BDNF is particularly interesting in that the spinal expression of this gene is strongly regulated to control pain sensitivity after limb injury and chronic opioid exposure (Li et al., 2008; Liang et al., 2014). The mechanism for up-regulation of spinal BDNF expression in these settings appears to involve the epigenetic acetylation of histone protein at the H3K9 mark leading to enhanced gene transcription. More broadly, epigenetic changes in the setting of TBI were recently reviewed with the conclusion that they likely participate in modulating multiple long-term consequences of TBI (Wong and Langley, 2016).

To begin our studies we characterized TBI-induced bleeding and blood-brain barrier breakdown after lateral fluid percussion (LFP) injury. We went on to examine the hypothesis that test agents able to block histone acetylation would reduce the severity and duration of nociceptive sensitization after TBI and that histone deacetylase inhibitors would have opposite effects. Further, we expected to observe that animals with dual TBI and hindpaw injuries, a model of polytrauma, might also respond to inhibitors of histone acetylation.

2. Methods

2.1. Animals

All experiments were approved by the Veterans Affairs Palo Alto Health Care System Institutional Animal Care and Use Committee (Palo Alto, CA, USA) and followed the animal subjects guidelines of the National Institutes of Health Guide for the Care and Use of Laboratory Animals. Male Sprague–Dawley rats (300 ± 20 g) from Harlan (Indianapolis, IN, USA) were used in these experiments. The animals were housed individually in 30 × 30 × 19-cm isolator cages with solid floors covered with 3 cm of wood chip bedding, and were given food and water *ad libitum*. Animals were kept under standard conditions with a 12-h light–dark cycle (6 a.m.–6 p.m.). All in vivo experiments were performed between 10 a.m. and 4 p.m. in the Veterinary Medical Unit. Separate groups of animals were used for behavioral, biochemical and immunohistochemical tests.

2.2. TBI surgery

A modification of the lateral fluid percussion (LFP) rat model of TBI was used as described previously (McIntosh et al., 1989; Ling et al., 2004; Feliciano et al., 2014). Rats were anesthetized using isoflurane inhalation and secured prone in a stereotactic frame. A midline incision was made in the scalp, and underlying periosteum removed. A 5 mm craniotomy was made in the rat skull using a mini-drill with a trephination bit. The craniotomy was placed midway between the bregma and lambda sutures, and centered approx. 2 mm to the right of the midline suture. The bone flap was moved under the adjacent scalp aiding preservation during the TBI procedure. Using cyanoacrylate glue, a female luer attachment was affixed to the craniotomy opening. Dental acrylic was then applied to the exposed rat skull to secure the instrumentation. Following recovery, the luer attachment was connected to the lateral fluid percussion apparatus (Amscien Instruments, USA), and a pressure wave of 1.3, (±0.1 atm) to produce mild level injuries or no pressure wave (sham) was applied to rat dura based on previous reports (McIntosh et al., 1989; Kabadi et al., 2010; McMahon et al., 2010). Thereafter, the luer attachment and dental acrylic were removed, the bone flap replaced and the overlying wound closed using 4-0 silk suture. Both TBI and sham rats were allowed to recover in their home cages.

2.3. Incision pain model

Some rats received hindpaw incisions using a modification of the plantar incisional pain model described by Brennan et al. as we described previously (Li et al., 2001). Briefly, rats were anesthetized using isoflurane 2–3% delivered through a nose cone. After sterile preparation with alcohol, a 1-cm longitudinal incision was made through the skin, muscle and fascia of the plantar foot with a number 11 scalpel blade contralateral to TBI. The incision was started 5 mm from the proximal edge of the heel and extended towards the toes. The underlying plantaris muscle was elevated with curved forceps and divided longitudinally, leaving the muscle origin and insertion intact. After controlling bleeding, two 6–0 nylon sutures were placed to approximate the wound edges and antibiotic ointment was applied.

2.4. Drug administration

Suberoylanilide hydroxamic acid (SAHA, Cayman Biochemical, Ann Arbor, Michigan), and curcumin (Sigma Chemical, St. Louis, MO) were freshly dissolved in DMSO and diluted in 0.9% saline (final DMSO concentration 10%). For curcumin treatment, animals received curcumin (50 mg/kg) or vehicle daily via subcutaneous (s.c.) injection into the loose skin of the back for seven days beginning immediately after surgery. The dosage of curcumin, a clinically available non-selective HAT inhibitor, was based on other's recent results (Zhu et al., 2014). For SAHA treatment, animals received SAHA 50 mg/kg or vehicle, daily via intra-peritoneal (i.p.) injection for 10days beginning immediately after surgery. This is a highly selective HDAC inhibitor. The dosage of this compound was based on our previous study (Liang et al., 2013; Sun et al., 2013). The injection volumes were 100 μl.

2.5. Behavioral testing

Neurological severity score - Neurological performance was assessed using a neurological severity score (NSS) as described previously (Feliciano et al., 2014). Rats were assessed and scored for each deficit in several categories for a maximal score of 24: (1) inability to exit a 50 cm circle, (2) righting reflex, (Renthal et al.) hemiplegia, (4) flexion of hind limbs when raised by tail, (5) inability to walk straight (6) reflexes (pinna/corneal/startle), (7) prostration, (8) loss of placing reflexes, (9) balance on stationary beam, and (10) failure in beam walking. Testing was completed at 1 and 7 days after injuries.

Mechanical allodynia - Mechanical withdrawal thresholds were measured using a modification of the up-down method and von Frey filaments as described previously (Guo et al., 2004). Animals were placed on wire mesh platforms in clear cylindrical plastic enclosures of 20 cm diameter and 30 cm in height. After 30 min of acclimation, fibers of sequentially increasing stiffness with initial bending force of 4.31N were applied to the plantar surface of the hind paw between the tori, and left in place 5 s with enough force to slightly bend the fiber. Withdrawal of the hind paw from the fiber was scored as a response. When no response was obtained, the next stiffer fiber in the series was applied in the same manner. If a response was observed, the next less stiff fiber was applied. Testing proceeded in this manner until 4 fibers had been applied after the first one causing a withdrawal response, allowing the estimation of the mechanical withdrawal threshold using a curve fitting algorithm (Poree et al., 1998). Testing was performed prior to injuries, and at intervals no more frequently than daily for up to 56 days. All the measurements were performed by the same person who was blind to the treatments.

2.6. Immunohistochemistry

The techniques employed for immunohistochemical analysis of spinal cord and brain tissue were based on those described previously by our group (Sun et al., 2013). Briefly, the lumbar spinal cords and brains were fixed in 4% paraformadehyde for 24 h. Then tissue was incubated in 0.5 M sucrose in phosphate buffered saline overnight, mounted in Tissue-Tek OCT embedding compound (Sakura Finetek), frozen. The spinal cords were cut into 10 μm sections from the L3 to L5 segments and the brains were cut into 40 μm sections from the olfactory bulbs to the medulla.

Blocking of the sections took place at 4 °C for 1 h in phosphate buffered saline containing 10% normal donkey serum, followed by exposure to the primary antibodies including rabbit anti-acetylated histone H3K9 antibody (1:500, Millipore) and mouse anti-NeuN (1:300, Millipore) overnight at 4 °C. Sections were then rinsed and incubated with fluorescein-conjugated secondary antibodies against the primary antibodies (1:500, Jackson ImmunoResearch Laboratories, West Grove, PA) for 1 h. Double-labeling immunofluorescence was performed with donkey anti-mouse IgG conjugated with cyanine dye 3, or donkey anti-rabbit IgG conjugated with fluorescein isothiocyanate secondary antibodies. Confocal laser-scanning microscopy was carried out using a Zeiss LSM/510 META microscope (Thornwood, NY). The IgG antibody for BBB breakdown was visualized by the DAB method (Vector Laboratories, CA, USA). Sections were pre-treated with 0.3% hydrogen peroxide in PBS for 30 min to quench endogenous peroxidases. Sections were blocked with 10% normal goat serum, and then incubated with biotin-conjugated goat anti-IgG (Vector Laboratories). This was followed by incubation with the Vectastain Elite ABC reagent (Vector Laboratories) and developed using the DAB peroxidase substrate kit (Vector Laboratories). Sections from control and experimental animals were processed in parallel. Control experiments omitting either primary or secondary antibody revealed no significant staining. Prussian blue iron staining was performed using freshly prepared 5% potassium hexacyanoferratetrihydrate (Sigma-Aldrich, MO, USA) and 5% hydrochloric acid (Sigma-Aldrich). Thirty min later, sections were rinsed in water and counterstained with nuclear fast red, dehydrated, and coverslipped using permount (Fisher Scientific, NH, USA).

The numbers of immune-target positive cells were counted in randomly selected superficial dorsal horn high-power fields (HPF, 400×) using 2-3 slices per animal, and 4 animals were included in each group. Results from all counts for sections from each individual group were combined prior to statistical analysis. Blinding of the observer was maintained until counting was completed.

Slides with IgG and Prussian blue were scanned at 1200 dpi using an Epson perfection V39 flatbed scanner (Epson America Inc, CA, USA) and analyzed using the NIH ImageJ program. For IgG quantification, sections from an uninjured, untreated rat were used to establish a threshold level that excluded all non-specific staining. This threshold level was then applied to all experimental groups. Both the area of the ipsilateral and contralateral sides and the % area of the sides that were positive for the IgG signal were quantified for each section. Results were expressed as the fold of IgG expression above that of untreated and uninjured controls. Assessment of Prussian blue stained sections involved quantification of the area of the ipsilateral and contralateral sides and the % area that was positive for blue deposits.

2.7. Circulating biomarkers of brain injury

For analysis of TBI biomarkers, serum samples were collected from TBI, TBI + Curcumin, TBI + SAHA, and sham control animals at day 7 after TBI. Rats were deeply anesthetized prior to blood draw with 3% isoflurane. The chest cavity was then opened, and 4–5 mL blood was collected from the heart using cardiac puncture. Samples were maintained at room temperature (RT) for 60 min and then centrifuged at 1500G for 10 min. The supernatant was extracted and immediately frozen on dry ice then stored at −80 °C prior to use.

ELISA assays were used to measure serum levels of selected biomarkers. Rat glial fibrillary acidic protein (GFAP), neuron-specific enolase 2 (NSE), and myelin basic protein (MBP) concentrations were measured in duplicate using rat GFAP, NSE, and MBP ELISA kits (LifeSpan Biotech), and rat calcium binding protein B (S100β) levels were assayed using an ELISA kit from MyBioSource according to the manufacturer's instructions. The biomarker levels were normalized by total protein concentration (Bio-Rad).

2.8. Statistical analysis

For multiple group comparisons, 2-way repeated-measure analysis of variance (ANOVA) followed by Newman-Keuls or Tukey post-hoc testing was employed. For the analysis of serum ELISA results, the concentration was normalized by total protein concentration. Prism 5 (GraphPad Software) was used for statistical calculations. Significance was set as $p < 0.05$. Data are presented as mean values ± standard error of the mean (SEM).

3. Results

3.1. Severity of neurological injury

To define the level of neurological impairment after LFP injury, we used the NSS. In Fig. 1 it can be seen that the TBI animals trended towards a slight degree of impairment 24 h after injury (not significant), but appeared to be very similar to sham operated animals by day 7. Therefore, it appears the TBI protocol results in mild injuries that are unlikely to interfere with the selected behavioral measurements.

3.2. Neuropathological analysis of LFP TBI animals

To define further the severity of brain injury in the LFP rats we studied the extravasation of IgG, a measure of blood-brain barrier (BBB) leakage, and the occurrence of microbleeds in the brains of LFP rats 7 days after injury. Reduced BBB integrity can compromise

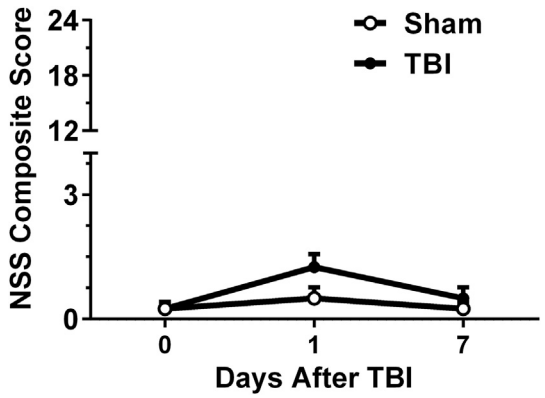

Fig. 1. Neurological severity score after sham or TBI. The LFP method was used to induce TBI using 1.3 atm pressure. The composite score ranges from 0 (no impairment) to 24 (maximal impairment). Data are presented as median with interquartile range. No significant differences were identified using the Mann-Whitney test. N = 8 rats/cohort.

the immune privileged status of the CNS and enhance inflammation (Kadota et al., 2000).

At 7 days post-injury, significant IgG accumulation could be detected ipsilateral to TBI, compared with uninjured rats (Fig. 2). Furthermore, the IgG signal was significantly greater when compared to that present in the contralateral side of the injured brain. Much of the IgG signal dissipated with distance from the injury site. The data in Fig. 3 show the appearance of hemosiderin staining that was confined to the ipsilateral side of the injured rat brain. There was no evidence of bleeding in the uninjured rats. In general, these findings were mild in nature and mostly confined to brain areas close to the site of injury.

3.3. Nociceptive sensitization after TBI

We next characterized the degree and duration of nociceptive sensitization caused by LFP. We followed nociceptive sensitization using von Frey filaments applied to the ipsilateral or contralateral hindpaws beginning prior to injuries and extending 8 weeks after exposing the animals to sham and TBI. The data in Fig. 4 show that TBI-induced mechanical allodynia in the contralateral hindpaws reached maximal severity by 2 days after injury and lasted approximately 3 weeks. Ipsilateral hindpaws showed a lower degree of sensitization than did hindpaws contralateral to TBI after injuries. No effect of sham surgery was observed in comparison to baseline sensitivity for the entire period of observation.

3.4. The influence of peripheral injury on TBI-induced nociceptive sensitization

Patients sustaining TBI often have coexisting somatic injuries such as occur in the setting of battlefield trauma or in motor vehicle accidents. To model these scenarios, we combined TBI with a well characterized rat hindpaw incision pain model (Brennan et al., 1996; Li et al., 2001). The data in Fig. 5 show that incision causes nociceptive sensitization lasting 7 days with recovery to baseline threshold values. When TBI was combined with incision, mechanical sensitization resembled that seen with TBI alone at later time points. Combining TBI and incision did not lead to more profound or longer duration sensitization than TBI alone.

3.5. Effects of curcumin on injury-induced allodynia

Histone acetylation is a major mechanism governing neuroplasticity. Previous laboratory studies have shown that the activation of histone acetyltransferase (HAT) activity is required for maximal sensitization and duration of allodynia after incision and other injuries (Sun et al., 2013). Using curcumin, a non-selective but clinically well-characterized HAT inhibitor, we determined the likely contributions of HAT to nociceptive sensitization after TBI, incision or the combination of injuries. We used this compound at a dose of 50 mg/kg, a dose shown previously to have large effects on sensitization after hindpaw incision alone (Sun et al., 2013). In Fig. 6A it is shown that the administration of curcumin beginning just after incision reduces the degree of sensitization after hindpaw incision. No effect on nociceptive sensitivity in control animals was observed. Nociceptive measurements were made immediately prior to daily curcumin administration to avoid measuring the acute effects of the drug. Fig. 6B shows that curcumin reduced the mechanical sensitization seen after TBI as well. Despite significant effects in each of the individual models, the data in Fig. 6C show that curcumin did not significantly alter the degree of mechanical sensitization observed after the combination of TBI and incision.

3.6. Effects of HDAC inhibition on nociceptive sensitization after TBI

Histone deacetylation reverses the effects of HAT, thus inhibition of HDAC enzymes was hypothesized to have effects opposite to curcumin in regulating nociceptive sensitization after TBI. Using a dose of the selective and clinically available HDAC inhibitor SAHA shown previously to prolong sensitization after hindpaw incision (Sun et al., 2014), we administered the HDAC inhibitor after inducing TBI. In Fig. 7 data are presented showing that SAHA administration beginning immediately after TBI causes the prolongation of hindpaw sensitization in comparison to TBI alone, although all animals tested recovered by 8 weeks of testing. Nociceptive measurements were made immediately before daily drug administration in order to quantify sustained effects.

3.7. The effects of TBI on spinal cord histone acetylation

The acetylation of histone proteins is a key epigenetic event altering gene transcription. Acetylation of the H3K9 mark is well-studied in association with pain and neuroplasticity within the CNS more broadly. We therefore harvested spinal cord tissue from sham and TBI animals 2 and 7 days after injury. The number of cells staining positively for AcH3K9 was quantified in dorsal horn lamina I and II of the lumbar spinal cord ipsilateral and contralateral to TBI. In Fig. 8 data are presented showing the increase in AcH3K9 in this sensory processing area. Ipsilateral changes appeared to lag contralateral changes in these studies.

We then determined whether the AcH3K9 in spinal cord tissue from mTBI animals was located in neurons as has been reported for models of nociceptive sensitization due to chemotherapeutic agents and chronic opioid exposure (Liang et al., 2014; Li et al., 2015). The micrographs in Fig. 8 demonstrate a strong co-localization of AcH3K9 with NeuN, a neuronal marker. Quantification of sections harvested on day 2 after mTBI revealed that 83.5 ± 1.0 percent of AcH3K9 positive cells also expressed the NeuN marker, indicating that the AcH3K9 is predominantly located in neurons.

3.8. Alteration of circulating biomarkers after TBI

Changes in levels of circulating CNS proteins in the serum of animal models and in some cases humans are used as indices of TBI

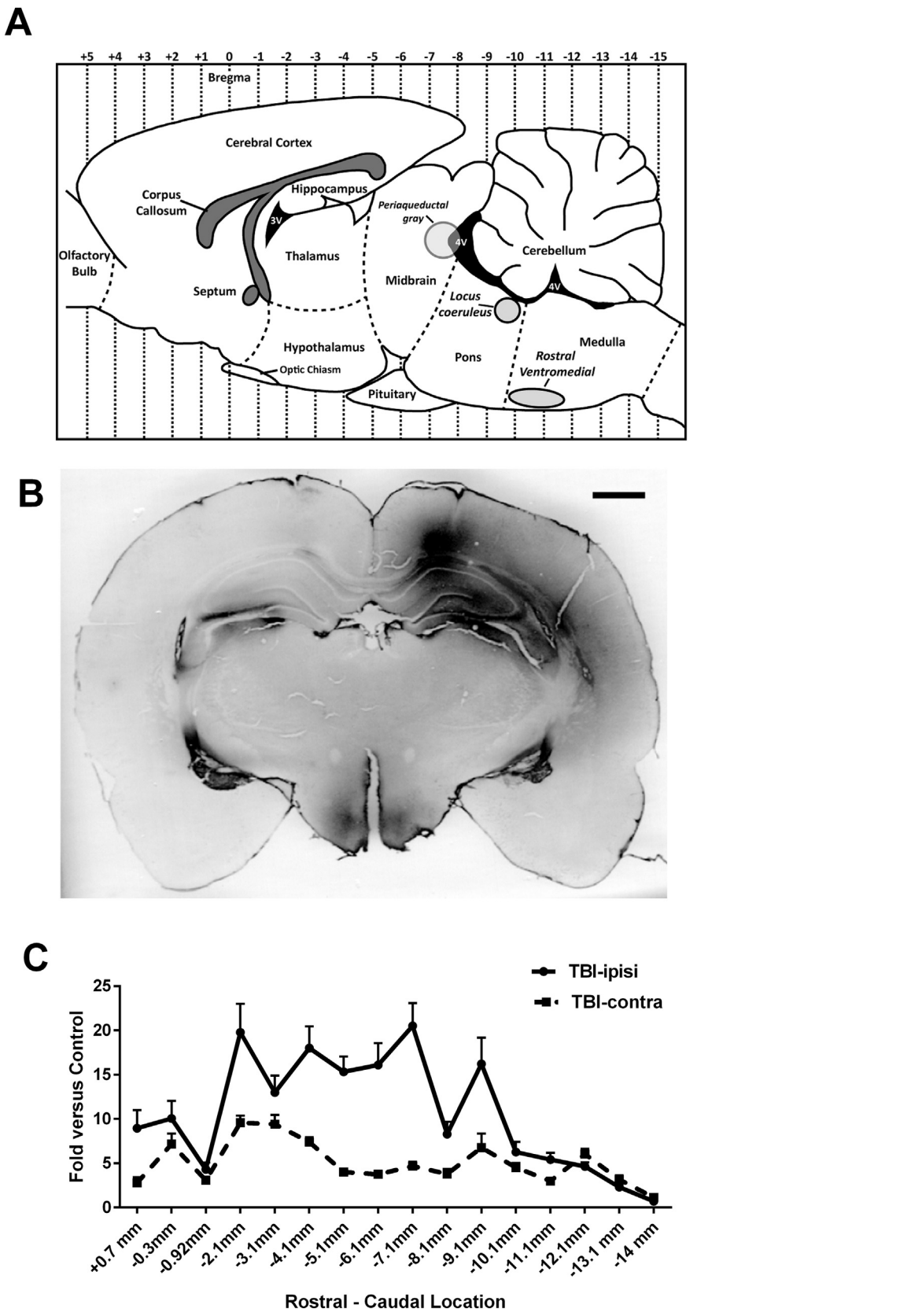

Fig. 2. Measure of blood-brain barrier (BBB) leakage with the extravasation of IgG. A: A schematic diagram of the rat brain in saggital section depicting the location of the supraspinal pain centers along the anterior-posterior axis. B: A representative photomicrograph of a rat brain at 7 days post-injury stained with an IgG antibody to demonstrate the extent of blood brain barrier breakdown. C: Graph depicts quantification of IgG staining across the anterior-posterior axis of the injured brain. Contra: contralateral side to TBI surgery site; Ipisi: Ipisilateral side to TBI surgery site. Scale bar = (B) 1 mm.

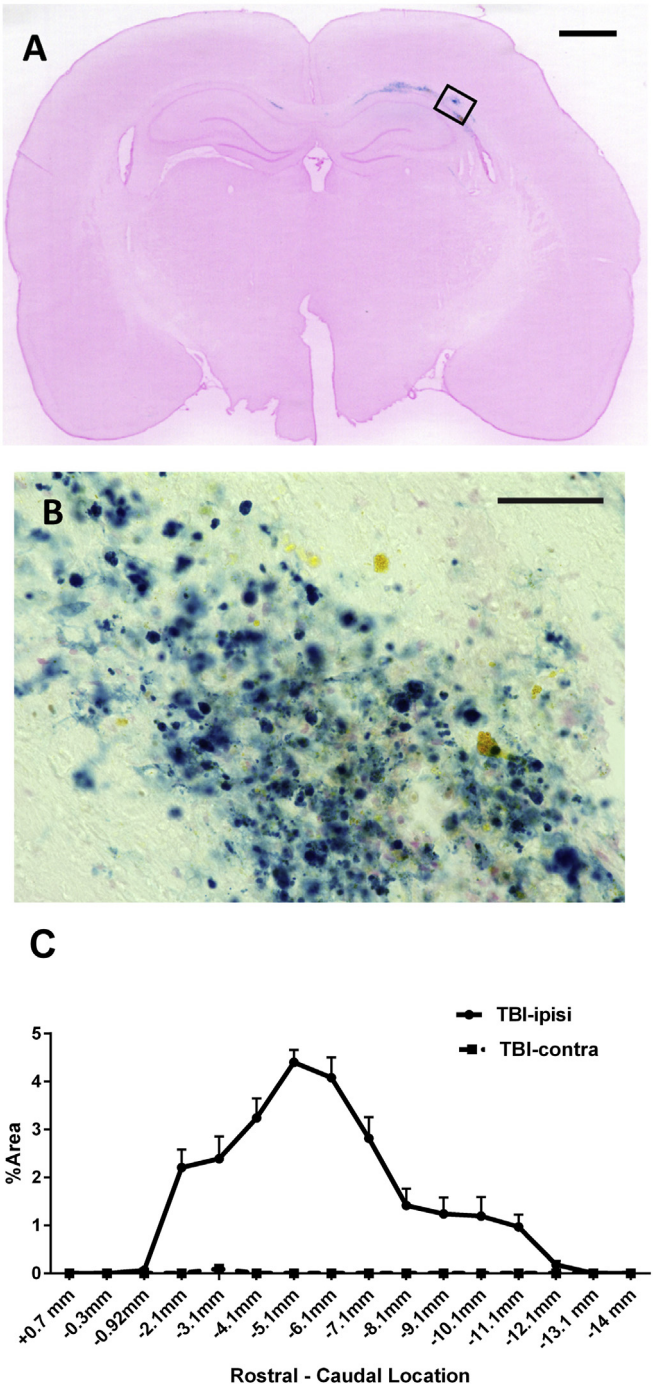

Fig. 3. Appearance of hemosiderin staining with iron deposits. A: A representative image of a Prussian blue stained brain section (A-P −5.0 mm) for iron deposi-tion at 7 days post-injury. Black box indicates location of B. B: A photomicrograph of iron deposits (blue) within the callosal radiations. C: Graph depicts quantification of iron deposits across the anterior-posterior axis of the injured brain. Contra: contralateral side to TBI surgery site; Ipisi: Ipisilateral side to TBI surgery site. Scale bar = (A) 1 mm and (B) 25 μm. (For interpretation of the references to colour in this figure legend, the reader is referred to the web version of this article.)

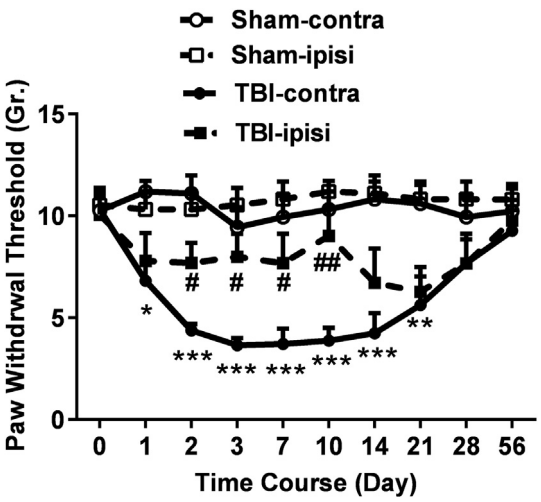

Fig. 4. Nociceptive sensitization after lateral fluid percussion. Animals received lateral fluid percussion force injuries at 1.3 atm on the right side of brain during the TBI procedure. Contra: contralateral side to TBI surgery site; Ipisi: Ipisilateral side to TBI surgery site. Nociceptive sensitivity at the indicated time points was measured using the von Frey method. The data were expressed as mean ± SEM. N = 6 rats/cohort. $^{*}p < 0.05$, $^{**}p < 0.01$, $^{***}p < 0.001$ comparison of contralateral sham to contralateral TBI paws. $^{\#}p < 0.05$, $^{\#\#}p < 0.01$, $^{\#\#\#}p < 0.001$ comparison of ipsilateral sham to ipsilateral TBI paws.

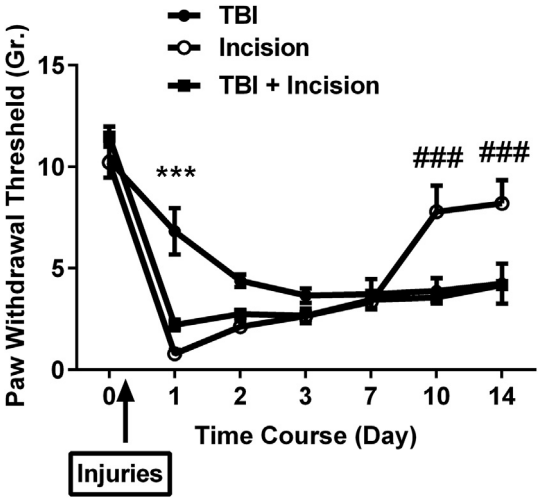

Fig. 5. Nociceptive features of TBI combined with peripheral trauma. Animals received paw incision or sham surgery controlateral to the side of TBI immediately after TBI was completed. Nociceptive sensitivity at the indicated time points was assessed using the von Frey method. Threshold values are displayed as means ± SEM. N = 6 rats/cohort. $^{***}p < 0.001$ comparison of TBI to incision groups. $^{\#\#\#}p < 0.001$ comparison of incision to TBI plus incision groups.

severity. We sought to determine whether the drugs used in these studies altered serum levels of these proteins which might indicate effects of the drugs on injury severity rather than pain signaling mechanisms as an explanation for our behavioral observations. Glial fibrillary acidic protein (GFAP), neuron-specific enolase 2 (NSE), myelin basic protein (MBP) and S100β levels were measured to broadly assess the severity of neuronal injury (Berger et al., 2007; Andruszkow et al., 2013; Egea-Guerrero et al., 2013; Papa et al., 2014; Schroeter et al., 2015). As presented in Fig. 9, it was shown that GFAP and NSE were significantly elevated at one week after TBI. Curcumin treatment did not change the serum levels of any of the markers tested from baseline or post-TBI levels. On the other hand, SAHA administration had mixed effects and was associated with a statistically significant enhancement of S100β above the levels. There were trends towards greater elevations of NSE and MBP in TBI animals also receiving SAHA though these changes did not achieve significance. Overall no consistent evidence of

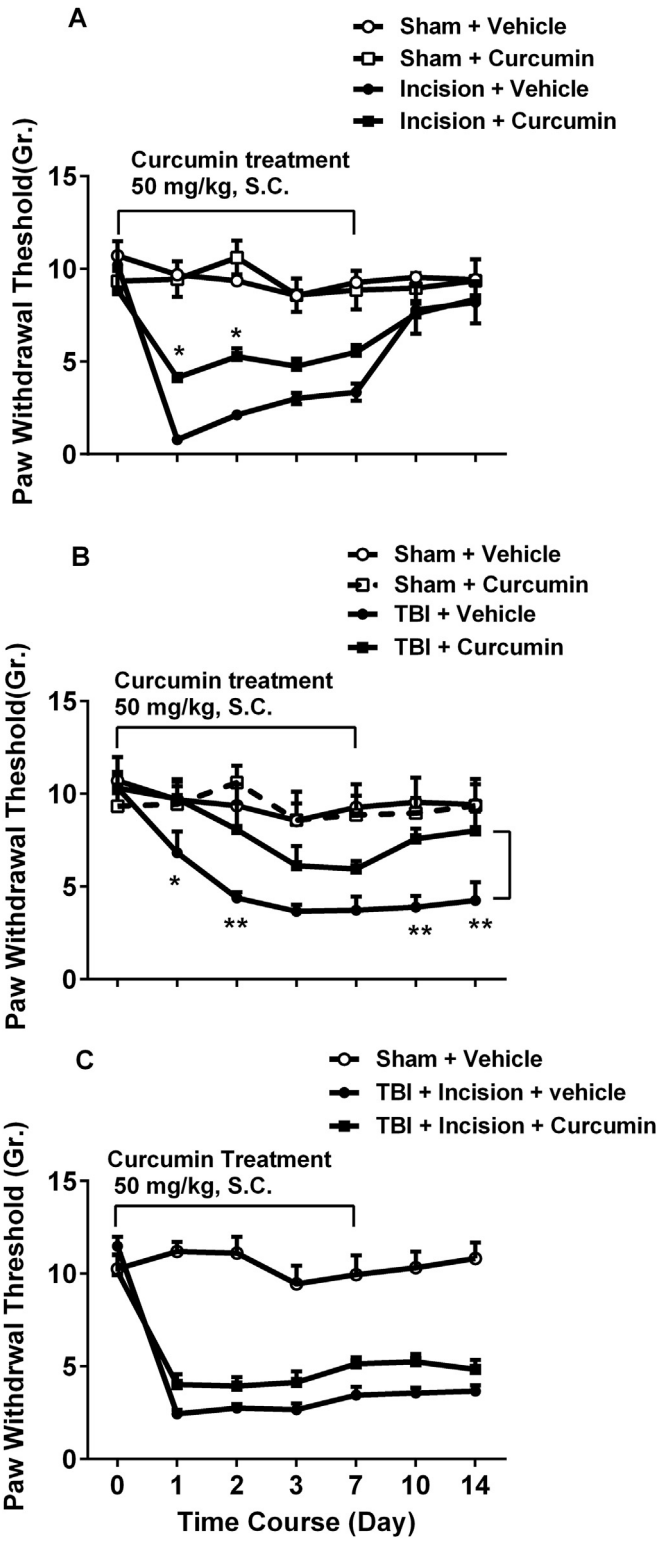

Fig. 6. Effects of curcumin on TBI and incision-induced nociceptive sensitization. Curcumin (50 mg/kg) was injected subcutaneously daily from day 0 to day 7 beginning immediately after injuries. Nociceptive sensitivity was assessed using von Frey fibers daily prior to daily curcumin injections. A: Effects of curcumin on incisional sensitization; B: Effects of curcumin on TBI-related sensitization in contralateral hindpaws. C: Effects of curcumin on animals with both TBI and hindpaw incisions. Threshold values are displayed as the mean ± SEM. N = 6 rats/cohort. $^{*}p < 0.05$, $^{**}p < 0.01$, comparison of contralateral paws in vehicle treated rats to the paws of curcumin treated animals.

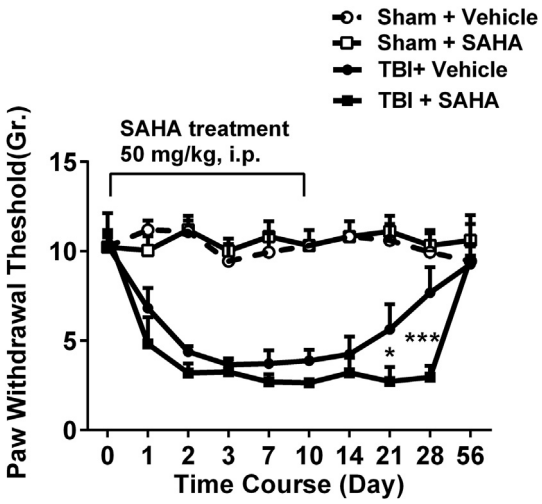

Fig. 7. Effects of SAHA on TBI-induced nociceptive sensitization. SAHA (50 mg/kg, i.p.) was injected daily from day 0 to day 10 beginning immediately after TBI. Nociceptive sensitivity was assessed using von Frey fibers before daily SAHA injections during the treatment period. Threshold values are displayed as mean ± SEM. N = 6 rats/cohort. $^{*}p < 0.05$, $^{**}p < 0.01$ comparison of TBI + vehicle to TBI + SAHA groups.

alteration in biomarkers secondary to the administration of the selected drugs was found.

4. Discussion

Traumatic brain injury (TBI), most frequently mild, accompanies battlefield, motor vehicle and sports-related injuries, and is often associated with chronic pain. More broadly, over 5 million Americans are living with TBI, many of whom experience chronic pain (Langlois et al., 2006). Chronic pain in the setting of TBI contributes to disability, causes suffering, complicates rehabilitative efforts and poses a significant overall challenge to management teams (Lippa et al., 2015). Unfortunately very little information is available concerning why patients with TBI develop chronic pain, and we have no specific treatments for TBI-related pain. Our studies confirm and extend previous human and animal analyses suggesting that mild traumatic brain injury unassociated with persistent neurological deficits can none-the-less support sensitization to painful or noxious stimuli. Moreover, the persistent nature of pain after TBI as well as recent observations of enhanced BDNF expression in the spinal cords of rats (Feliciano et al., 2014) and non-human primates (Nagamoto-Combs et al., 2007) suggests epigenetic mechanisms might be activated at sites distant from the TBI even after mild injuries. The regulation of histone acetylation in neural tissues is a known mechanism regulating the persistence of nociceptive sensitization after hindpaw incision, inflammation and nerve damage (Chiechio et al., 2009; Bai et al., 2010; Sun et al., 2013; Liang et al., 2014, 2015). Our studies demonstrate that well-characterized pharmacological treatments either diminishing (curcumin) or enhancing (SAHA) the level of histone acetylation are in fact able to regulate nociceptive sensitization after TBI or hindpaw incision. Furthermore, TBI increased the spinal abundance of acetylated H3K9 in spinal cord neurons complementing our earlier findings that hindpaw incision increases acetylated H3K9 in neurons from the same sensory processing regions of the spinal cord (Sun et al., 2013). Our data do not, however, exclude the involvement of glial cells in the spinal response to TBI.

Our analyses demonstrated that TBI as carried out in these experiments caused only small and transient effects on the Nuerological Severity Scale (NSS), limited breakdown of the blood-brain

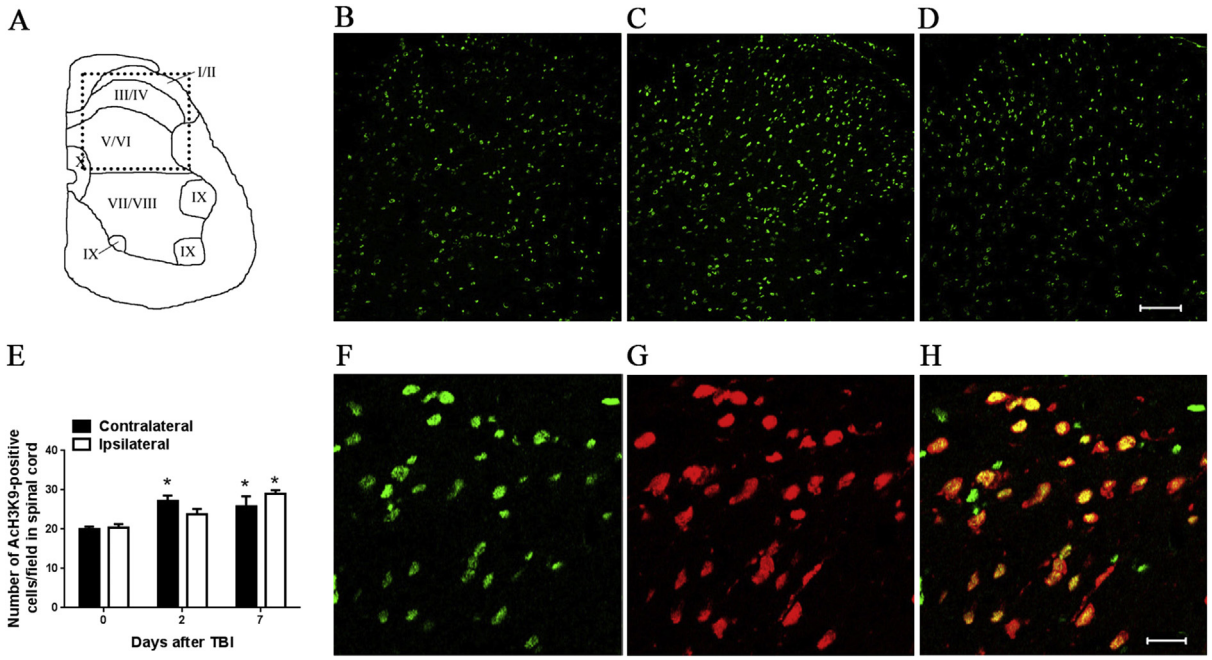

Fig. 8. TBI increases the number of AcH3K9 expressing cells in the lumbar spinal cord dorsal horn. (A) Cytoarchitecture of the rodent lumbar spinal cord. The dotted line indicates the dorsal horn region displayed in panels B–D. Immunostaining showed that AcH3K9 was expressed in the dorsal horn of contralateral spinal cord in normal control rats (B) and at 2 days (C) and 7 days after TBI (D). Panels B–D scale bar = 100 μm. (E) Quantification of AcH3K9 positively staining cells in the dorsal horn areas of the spinal cord. n = 3, *p < 0.05, versus individual baseline. Double staining for AcH3K9 (F) and NeuN markers (G) demonstrates strong association with AcH3K9 in neuronal cells (H) in contralateral spinal cord dorsal horn tissue 2 days after TBI. Panels F–H scale bar = 20 μm.

barrier and limited intraparenchymal bleeding. Similarly, others have reported BBB damage in the cortex, hippocampus and other areas in the rat LFP model (Stein et al., 2009). Furthermore, our survey of serum markers of injury severity did identify elevations of

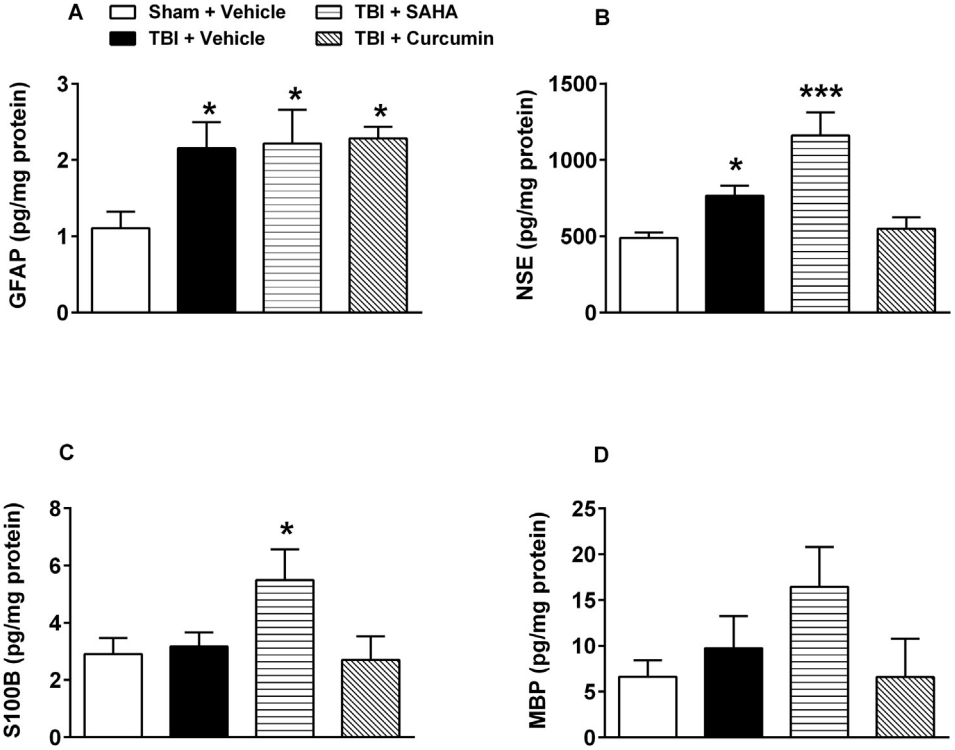

Fig. 9. Alteration of circulating biomarkers after TBI. Serum levels of (A) glial fibrillary acidic protein (GFAP), (B) neuron-specific enolase (NSE), (C) S100 calcium binding protein B (S100B), or (D) myelin basic protein (MBP) 7 days after TBI injuries. Animals were treated with vehicle, curcumin or SAHA as described in Materials and Methods. The values are displayed as mean ± SEM. N = 6 rats/cohort. *p < 0.05, ***p < 0.001 comparison of TBI-sham groups with TBI + vehicle, TBI + curcumin or TBI + SAHA group.

some of the proteins, but these were not systematically altered by the epigenetic test agents. Therefore our results are not easily attributable to gross drug-induced changes in the brain injuries themselves. Rather, it may be more likely that functional changes in brain and spinal tissue explain the nociception-related changes.

Epigenetics is a field of science involving the study of persistent changes in gene expression or cellular phenotype caused by mechanisms apart from changes in DNA sequence (Bird, 2007). Some of the most important epigenetic modifications related to complex diseases are DNA methylation and acetylation of histone proteins on specific lysine residues. The acetylation of histone proteins by histone acetyl transferase (HAT) enzymes such as CBP/P300, GNATs and MYST proteins causes relaxation of chromatin structure and enhanced gene transcription while histone deacetylases (HDAC's) reduce transcription through DNA condensation. Interest in epigenetics in the pain research community has grown rapidly as these mechanisms may constitute novel chronic pain master switches (Doehring et al., 2011). For example, HDAC inhibitors administered intrathecally regulate the hyperalgesia induced by hindpaw injection of Complete Freund's Adjuvant (CFA) (Bai et al., 2010). Our own previous work suggested that blockade of HAT activity using anacardic acid can reduce nociceptive sensitization after hindpaw incision, likely by altering spinal histone acetylation (Sun et al., 2013). In models of neuropathic pain, histone acetylation in spinal cord tissue appears to control nociceptive sensitization (Bai et al., 2010; Sun et al., 2013; Zammataro et al., 2014; Liang et al., 2015). It should be noted, however, that while curcumin reduced mechanical nociceptive sensitization after TBI and incision in our rat model, this compound failed to reverse sensitization after the combination of TBI and paw incision. Explanations for these results include the possibility that the dosage of curcumin used was too low. Consistent with this possibility, a recent study reported that curcumin used at100 mg/kg and 200 mg/kg was able to suppress nociceptive sensitivity induced by CFA injection, but not 50 mg/kg, the dose that we used (Chen et al., 2015). Relatedly, our subcutaneous as opposed to intrathecal administration of curcumin post-injury may not provide adequate CNS levels of the drug to cause maximal effects. Another possibility is that epigenetic changes play a limited role in nociceptive sensitization when TBI is combined with hidpaw incision. Thus while clinically safe (Jantan et al., 2015; Oliveira et al., 2015; Peddada et al., 2015), curcumin and other HAT inhibitors might not have the efficacy required to overcome sensitization when multiple injuries are experienced.

While our pharmacological data suggest histone acetylation may regulate nociceptive sensitization after TBI and peripheral injury as often clinically co-exist, we did not focus specifically on the likely genes being regulated. In fact, it needs to be kept in mind that epigenetic mechanisms typically groups of genes rather than individual ones. In the case of TBI it appears the balance of gene regulation favors a pro-nociceptive state. Several genes regulated by histone acetylation in the vicinity of their promoters may individually or collectively support nociceptive sensitization. The BDNF gene was already mentioned as one possibility. This gene when expressed by sensory neurons, intrinsic spinal cord neurons or glial cells acts through the TrkB receptor to facilitate nociceptive signaling. For example, we recently demonstrated that the hyperalgesia caused by chronic exposure to opioids enhances mechanical allodynia in spinal TrkB-dependent fashion with epigenetically up-regulated BDNF from dorsal horn neurons being the apparent source of this neurotrophin (Liang et al., 2014). Likewise Zhu et al. provided evidence that spinal BDNF was epigenetically up-regulated, supporting neuropathic sensitization, and that this could be blocked by curcumin administration (Zhu et al., 2014). It was observed in a recent analysis of NK1 receptor expression in the brains of rats after TBI that significant up-regulation was present in both thalamic and cortical tissue (Mustafa et al., 2016), areas we noted to be damaged in our model. While not specifically explored in those studies, the expression of the NK1 gene is epigenetically controlled via the regulation of histone acetylation (Renthal et al., 2007). Additional studies have suggested PDYN, CX3CL1, Cdk5, CXCR2 and other epigenetically-regulated genes are up-regulated and support nociceptive sensitization in various pain models (Sun et al., 2013; Li et al., 2014, 2015; Liang et al., 2014; Li et al., 2015). Aside from offering a novel mechanism for a common comorbidity of TBI, new approaches to treatment are suggested by the demonstration of involvement of histone acetylation. Curcumin itself, a safe substance available as a health supplement, might be an option for those with TBI, particularly if new oral formulations with enhanced bioavailability become available (Douglass and Clouatre, 2015; Latimer et al., 2015; Patil et al., 2015; Zheng et al., 2015).

One additional finding of our studies consistent with some clinical reports is that limbs contralateral to brain injury demonstrated more profound and rapid nociceptive sensitization compared to contralateral limbs (Ofek and Defrin, 2007). We observed only very mild sensitization of limbs ipsilateral to TBI after mild percussive force. In pilot experiments using a stronger stimulus (1.7 atm) we did observe ipsilateral sensitization, but it was somewhat delayed in comparison the contralateral time course (data not shown). These data suggest that lateralized injuries may differentially affect nociceptive processing just as motor and other sequelae can be lateralized after TBI or other forms of brain injury.

Overall, this series of studies demonstrates that LFP-induced TBI produces nociceptive sensitization of contralateral hindlimbs in rats. These studies also provide presumptive evidence that epigenetic mechanisms underlie, at least in part, this sensitization. If similar mechanisms were found to operate in human TBI patients, these insights could lead to the development of novel treatments to reduce the severity or prevent the chronification of TBI-related pain. Thus, it is critical to further understand the mechanisms linking brain injury to changes in histone acetylation and to better define the set of pro-nociceptive genes responding to TBI that this acetylation modulates.

Conflicts of interest

The authors have no conflicts of interest to declare.

Acknowledgements

This work was supported by the DOD CDMRP award MR130295 to JDC.

References

Andruszkow, H., et al., 2013. Does additional head trauma affect the long-term outcome after upper extremity trauma in multiple traumatized patients: is there an additional effect of traumatic brain injury? Clin. Orthop. Relat. Res. 471, 2899–2905.

Bai, G., et al., 2010. Inhibition of class II histone deacetylases in the spinal cord attenuates inflammatory hyperalgesia. Mol. Pain 6, 51.

Berger, R.P., et al., 2007. Serum biomarker concentrations and outcome after pediatric traumatic brain injury. J. neurotrauma 24, 1793–1801.

Bird, A., 2007. Perceptions of epigenetics. Nature 447, 396–398.

Brennan, T.J., et al., 1996. Characterization of a rat model of incisional pain. Pain 64, 493–501.

Chen, J.J., et al., 2015. Intrathecal curcumin attenuates pain hypersensitivity and decreases spinal neuroinflammation in rat model of monoarthritis. Sci. Rep. 5, 10278.

Chiechio, S., et al., 2009. Epigenetic modulation of mGlu2 receptors by histone deacetylase inhibitors in the treatment of inflammatory pain. Mol. Pharmacol. 75, 1014–1020.

Coronado, V.G., et al., 2011. Surveillance for traumatic brain injury-related deaths–United States, 1997-2007. MMWR Surveill. Summ. 60, 1–32.
Doehring, A., et al., 2011. Epigenetics in pain and analgesia: an imminent research field. Eur. J. Pain 15, 11–16.
Douglass, B.J., Clouatre, D.L., 2015. Beyond yellow curry: assessing commercial curcumin absorption technologies. J. Am. Coll. Nutr. 34, 347–358.
Egea-Guerrero, J.J., et al., 2013. S100B protein may detect brain death development after severe traumatic brain injury. J. Neurotrauma 30, 1762–1769.
Faul, M., Coronado, V., 2015. Epidemiology of traumatic brain injury. Handb. Clin. Neurol. 127, 3–13.
Feliciano, D.P., et al., 2014. Nociceptive sensitization and BDNF up-regulation in a rat model of traumatic brain injury. Neurosci. Lett. 583, 55–59.
Guo, T.Z., et al., 2004. Substance P signaling contributes to the vascular and nociceptive abnormalities observed in a tibial fracture rat model of complex regional pain syndrome type I. Pain 108, 95–107.
Higgins, D.M., et al., 2014. Persistent pain and comorbidity among operation enduring freedom/operation iraqi freedom/operation new dawn veterans. Pain Med. 15, 782–790.
Hyder, A.A., et al., 2007. The impact of traumatic brain injuries: a global perspective. NeuroRehabilitation 22, 341–353.
Jantan, I., et al., 2015. Plant-derived immunomodulators: an insight on their preclinical evaluation and clinical trials. Front. Plant Sci. 6, 655.
Kabadi, S.V., et al., 2010. Fluid-percussion-induced traumatic brain injury model in rats. Nat. Protoc. 5, 1552–1563.
Kadota, E., et al., 2000. Biological functions of extravasated serum IgG in rat brain. Acta Neurochir. Suppl. 76, 69–72.
Lahz, S., Bryant, R.A., 1996. Incidence of chronic pain following traumatic brain injury. Arch. Phys. Med. Rehabil. 77, 889–891.
Langlois, J.A., et al., 2006. The epidemiology and impact of traumatic brain injury: a brief overview. J. Head. Trauma Rehabil. 21, 375–378.
Latimer, B., et al., 2015. Enhanced systemic bioavailability of curcumin through transmucosal administration of a novel microgranular formulation. Anticancer Res. 35, 6411–6418.
Li, C.Q., et al., 2008. Brain derived neurotrophic factor (BDNF) contributes to the pain hypersensitivity following surgical incision in the rats. Mol. Pain 4, 27.
Li, D., et al., 2015. Up-regulation of CX3CL1 via nuclear factor-kappaB-dependent histone acetylation is involved in paclitaxel-induced peripheral neuropathy. Anesthesiology 122, 1142–1151.
Li, K., et al., 2014. Epigenetic upregulation of Cdk5 in the dorsal horn contributes to neuropathic pain in rats. Neuroreport 25, 1116–1121.
Li, X., et al., 2001. Opioid-induced hyperalgesia and incisional pain. Anesth. Analg. 93, 204–209.
Liang, D.Y., et al., 2013. Epigenetic regulation of opioid-induced hyperalgesia, dependence, and tolerance in mice. J. Pain Off. J. Am. Pain Soc. 14, 36–47.
Liang, D.Y., et al., 2014. Epigenetic regulation of spinal cord gene expression controls opioid-induced hyperalgesia. Mol. Pain 10, 59.
Liang, L., et al., 2015. Epigenetic regulation of chronic pain. Epigenomics 7, 235–245.
Ling, G.S., et al., 2004. Traumatic brain injury in the rat using the fluid-percussion model. Curr. Protoc. Neurosci. (Chapter 9):9.2.1–9.2.11.
Lippa, S.M., et al., 2015. Deployment-related psychiatric and behavioral conditions and their association with functional disability in OEF/OIF/OND veterans. J. Trauma Stress 28, 25–33.
Macolino, C.M., et al., 2014. Mechanical alloydnia induced by traumatic brain injury is independent of restraint stress. J. Neurosci. Methods 226, 139–146.
McIntosh, T.K., et al., 1989. Traumatic brain injury in the rat: characterization of a lateral fluid-percussion model. Neuroscience 28, 233–244.
McMahon, C.G., et al., 2010. The effect of acute traumatic brain injury on the performance of shock index. J. Trauma 69, 1169–1175.
Mittenberg, W., et al., 1992. Symptoms following mild head injury: expectation as aetiology. J. Neurol. Neurosurg. Psychiatry 55, 200–204.
Murphy, M.P., Carmine, H., 2012. Long-term health implications of individuals with TBI: a rehabilitation perspective. NeuroRehabilitation 31, 85–94.
Mustafa, G., et al., 2016. Trigeminal neuroplasticity underlies allodynia in a preclinical model of mild closed head traumatic brain injury (cTBI). Neuropharmacology 107, 27–39.
Nagamoto-Combs, K., et al., 2007. Prolonged microgliosis in the rhesus monkey central nervous system after traumatic brain injury. J. neurotrauma 24, 1719–1742.
Nampiaparampil, D.E., 2008. Prevalence of chronic pain after traumatic brain injury: a systematic review. JAMA 300, 711–719.
Ofek, H., Defrin, R., 2007. The characteristics of chronic central pain after traumatic brain injury. Pain 131, 330–340.
Oliveira, A.S., et al., 2015. Curcumin: a natural lead for potential new drug candidates. Curr. Med. Chem. 22, 4196–4232.
Papa, L., et al., 2014. GFAP out-performs S100beta in detecting traumatic intracranial lesions on computed tomography in trauma patients with mild traumatic brain injury and those with extracranial lesions. J. neurotrauma 31, 1815–1822.
Patil, S., et al., 2015. Enhanced oral bioavailability and anticancer activity of novel curcumin loaded mixed micelles in human lung cancer cells. Phytomedicine 22, 1103–1111.
Peddada, K.V., et al., 2015. Role of curcumin in common musculoskeletal disorders: a review of current laboratory, translational, and clinical data. Orthop. Surg. 7, 222–231.
Poree, L.R., et al., 1998. The analgesic potency of dexmedetomidine is enhanced after nerve injury: a possible role for peripheral alpha2-adrenoceptors. Anesth. Analg. 87, 941–948.
Rao, V., et al., 2015. Neuropsychiatric disturbances associated with traumatic brain injury: a practical approach to evaluation and management. Semin. Neurol. 35, 64–82.
Renthal, W., et al., 2007. Histone deacetylase 5 epigenetically controls behavioral adaptations to chronic emotional stimuli. Neuron 56, 517–529.
Sayer, N.A., et al., 2009. Rehabilitation needs of combat-injured service members admitted to the VA Polytrauma Rehabilitation Centers: the role of PM&R in the care of wounded warriors. PM R. 1, 23–28.
Schroeter, M.L., et al., 2015. Serum neuron-specific enolase is related to cerebellar connectivity: a resting-state functional magnetic resonance imaging pilot study. J. neurotrauma 32, 1380–1384.
Stein, S.C., et al., 2009. Erythrocyte-bound tissue plasminogen activator is neuroprotective in experimental traumatic brain injury. J. Neurotrauma 26, 1585–1592.
Sun, Y., et al., 2014. Opioids enhance CXCL1 expression and function after incision in mice. J. Pain Off. J. Am. Pain Soc. 15, 856–866.
Sun, Y., et al., 2013. Epigenetic regulation of spinal CXCR2 signaling in incisional hypersensitivity in mice. Anesthesiology 119, 1198–1208.
Wong, V.S., Langley, B., 2016. Epigenetic changes following traumatic brain injury and their implications for outcome, recovery and therapy. Neurosci. Lett. 625, 26–33.
Zammataro, M., et al., 2014. HDAC and HAT inhibitors differently affect analgesia mediated by group II metabotropic glutamate receptors. Mol. Pain 10, 68.
Zheng, Z., et al., 2015. The effect of curcumin and its nanoformulation on adjuvant-induced arthritis in rats. Drug Des. Devel Ther. 9, 4931–4942.
Zhu, X., et al., 2014. Curcumin alleviates neuropathic pain by inhibiting p300/CBP histone acetyltransferase activity-regulated expression of BDNF and cox-2 in a rat model. PloS One 9, e91303.